Marine Chemistry 184 (2016) 11–20

Contents lists available at ScienceDirect

Marine Chemistry

journal homepage: www.elsevier.com/locate/marchem

The measurement of pH in saline and hypersaline media at sub-zero temperatures: Characterization of Tris buffers

Stathys Papadimitriou [a,*], Socratis Loucaides [b], Victoire Rérolle [b,c], Eric P. Achterberg [d,e], Andrew G. Dickson [f], Matthew Mowlem [b], Hilary Kennedy [a]

[a] Ocean Sciences, College of Natural Sciences, Bangor University, Menai Bridge LL59 5AB, UK
[b] National Oceanography Centre, Southampton SO14 3ZH, UK
[c] Sorbonne Universités (UPMC, Univ Paris 06)-CNRS-IRD-MNHN, LOCEAN Laboratory, 75005 Paris, France
[d] University of Southampton, National Oceanography Centre, Southampton SO14 3ZH, UK
[e] GEOMAR, Helmholtz Centre for Ocean Research, 24148 Kiel, Germany
[f] Marine Physical Laboratory, Scripps Institution of Oceanography, University of California, San Diego, 9500 Gilman Drive, La Jolla, CA 92093-0244, USA

ARTICLE INFO

Article history:
Received 23 December 2015
Received in revised form 3 June 2016
Accepted 8 June 2016
Available online 11 June 2016

Keywords:
Calibration
Standards
pH
Traceability
Sea ice
Brine
Low temperature

ABSTRACT

The pH on the total proton scale of the Tris-HCl buffer system (pH_{Tris}) was characterized rigorously with the electrochemical Harned cell in salinity (S) 35 synthetic seawater and S = 45–100 synthetic seawater-derived brines at 25 and 0 °C, as well as at the freezing point of the synthetic solutions (−1.93 °C at S = 35 to −6 °C at S = 100). The electrochemical characterization of the common equimolal Tris buffer [$R_{Tris} = m_{Tris}/m_{Tris\text{-}H^+} = 1.0$, with $m_{Tris} = m_{Tris\text{-}H^+} = 0.04$ mol $kg_{H_2O}^{-1}$ = molality of the conjugate acid-base pair of 2-amino-2-hydroxymethyl-1,3-propanediol (Tris)] yielded pH_{Tris} values which increased with increasing salinity and decreasing temperature. The electrochemical characterization of a non-equimolal Tris buffer variant (R_{Tris} = 0.5, with m_{Tris} = 0.02 mol $kg_{H_2O}^{-1}$ and $m_{Tris-H^+} = 0.04$ mol $kg_{H_2O}^{-1}$) yielded pH_{Tris} values that were consistently less alkaline by 0.3 pH unit than those of the equimolal Tris buffer. This is in agreement with the values derived from the stoichiometric equilibrium of the Tris-H^+ dissociation reaction, described by the Henderson – Hasselbalch equation, $pH_{Tris} = pK_{Tris}^* + \log R_{Tris}$, with pK_{Tris}^* = stoichiometric equilibrium dissociation constant of Tris-H^+, equivalent to equimolal pH_{Tris}. This consistency allows reliable use of other R_{Tris} variants of the Tris-HCl buffer system within the experimental conditions reported here. The results of this study will facilitate the pH measurement in saline and hypersaline systems at below-zero temperatures, such as sea ice brines.

1. Introduction

High latitude oceans contribute disproportionally to the CO_2 uptake from the atmosphere (Bates and Mathis, 2009; Takahashi et al., 2002), but these estimates are based on data generated by sampling ice-free parts of the polar oceans. A complete picture of the polar CO_2 budget must include the role of the seasonal and perennial sea ice in CO_2 cycling and air-sea exchange in these regions. Recent research has demonstrated that brine pockets in sea ice are sites of physical and biogeochemical processing that render sea ice an environment of active carbon cycling (Arrigo et al., 1997; Dieckmann et al., 2008; Gleitz et al., 1995; Miller et al., 2011a, 2011b; Munro et al., 2010; Papadimitriou et al., 2012; Rysgaard et al., 2011; Rysgaard et al., 2007). Processes, such as primary and secondary production (Arrigo et al., 1997; Deming, 2010), mineral authigenesis, including $CaCO_3$ in the form of ikaite (Dieckmann et al., 2010; Dieckmann et al., 2008; Rysgaard et al., 2013), gas exchange (Miller et al., 2011a, 2011b; Papadimitriou et al., 2012; Papadimitriou et al., 2004), and brine drainage (Notz and Worster, 2009) have dynamic seasonal cycles in sea ice and affect the carbonate system at the ocean-air interface in high latitudes (Bates and Mathis, 2009; Bates et al., 2006; Chierici and Fransson, 2009; Dieckmann et al., 2008; Fischer et al., 2013; Miller et al., 2011b; Papadimitriou et al., 2014; Papadimitriou et al., 2013; Rysgaard et al., 2012; Takahashi et al., 2002; Yamamoto-Kawai et al., 2011; Yamamoto-Kawai et al., 2009). However, in comparison with the current advancement of our knowledge on ice-free waters of the high latitude oceans, the study of the carbonate system in sea ice has been patchy, not least because of logistical and physical-chemical complexities (Miller et al., 2015).

Sea ice is a porous medium of mostly pure ice with a small percentage by volume of brine and gas pockets (Cox and Weeks, 1983). The chemical composition of the liquid and gas phases of sea ice results from the physical-chemical changes attendant on seawater freezing, its dissolved salt and gas expulsion from the pure ice matrix, and their entrapment and physical concentration in pockets within (Cox and Weeks, 1983). Thus, sea ice brines exhibit a much wider range of salinity

* Corresponding author.
E-mail address: s.papadimitriou@bangor.ac.uk (S. Papadimitriou).

http://dx.doi.org/10.1016/j.marchem.2016.06.002

(S) and temperature (t) within short temporal and spatial scales than the underlying and ice-free oceanic waters. The temperature of sea ice ranges from the freezing point of seawater at the ice-water interface [t_{fr} = −1.93 °C at 1 atm total pressure and S = 35; UNESCO (1983)] to temperatures as low as −16 °C, or even lower during winter, in the coldest upper parts of ice floes in contact with the atmosphere (Miller et al., 2011a, 2011b) accommodating hypersaline (S >>35) brines of an equivalent freezing point. For example, at −6 °C, about 66% of the water is present as ice and the residual brine has a salinity of 100. The temperature range where in situ investigation of the carbonate system in sea ice would be most beneficial is between the freezing point of seawater and the temperature at which the sea ice becomes impermeable to liquid transport and material exchange with the underlying ocean. This occurs when the brine volume becomes <5%, which occurs at −5 °C when bulk sea ice S = 5 (Golden et al., 1998).

For the investigation of the carbonate system under such S–t conditions as found in sea ice, total alkalinity (TA), total dissolved inorganic carbon (DIC), and dissolved CO_2 (as gas fugacity, fCO_2) measurements are possible using current methodologies and instrumentation (Miller et al., 2015) but not the measurement of pH, which is only possible thus far at above-zero temperatures and salinities up to 40. An estimate of the pH at the sub-zero temperatures and high salinities of sea ice brines can be computed from the solution of the thermodynamic model that describes the oceanic carbonate system using measurements of TA and DIC as input parameters (Brown et al., 2014; Delille et al., 2007; Gleitz et al., 1995; Papadimitriou et al., 2007; Papadimitriou et al., 2004). This requires knowledge of the dissociation constants of carbonic and boric acids at the salinity and temperature ranges of sea ice. Empirical data for these constants, however, do not exist for t < 0 °C and S > 50 in natural solutions (Dickson, 1990a; Millero et al., 2006). The required extrapolation to lower temperatures and higher salinities of the non-linear S–t functions that describe the existing empirical data set can result in sizeable errors in these computations (Brown et al., 2014). With this caveat in mind, the estimated in situ pH in sea ice brines has been reported to range between 7 and 10 (Delille et al., 2007; Gleitz et al., 1995; Miller et al., 2011a; Papadimitriou et al., 2007). Finally, the use of the traditional pH measurement techniques (potentiometry, spectrophotometry) at sub-zero temperatures and high salinities is challenging because of untested electrochemical behaviour of glass electrodes used in potentiometry, lack of experimental data for the optical parameters and dissociation constants of pH indicator dyes used in spectrophotometry, and lack of suitable calibration buffers compounding the uncertainties of both potentiometric and spectrophotometric methods at sub-zero temperatures and hypersaline conditions. The range of environmental conditions for which saline pH buffers have been characterized is 0–40 °C and S = 20–40 for the 2-amino-2-hydroxymethyl-1,3-propanediol (Tris) compound in synthetic seawater (DelValls and Dickson, 1998), as well as 5–45 °C and S = 35 for 2-amino-2-methyl-1,3-propanediol (Bis), tetrahydro-1,4-isoxazine (Morpholine), and 2-amino-pyridine (Aminopyridine) (Millero et al., 1993), all on the total proton scale. Similarly, pH indicator dyes have typically been characterized at above-zero temperatures and S < 40 conditions on the total and free proton scales (e.g., Liu et al., 2011; Robert-Baldo et al., 1985), with a further extension of the dye data set on the free proton scale in NaCl solutions by Millero et al. (2009) to the full ionic strength spectrum up to NaCl saturation (0.03 < I < 5.50 m) at above-zero temperatures. Overall, there is currently no validated method for measuring pH at sub-zero temperatures or, especially, in the coupled sub-zero temperature and high salinity of sea ice brines, or at any temperature for S > 40 in multi-electrolyte media.

The aim of this work was to enable reliable measurement of pH in saline and hypersaline media at sub-zero temperatures. To this end, we determined the pH of Tris buffer solutions in corresponding salinity and temperature conditions. For this task, we extended the standard electrochemical protocol for pH buffer characterization to international standards in the Harned (hydrogen gas/silver/silver chloride) cell (Bates, 1973) described in the oceanographic pH literature (Campbell et al., 1993; DelValls and Dickson, 1998; Dickson, 1990a, 1990b; Millero et al., 1993). The electrochemical characterization of pH buffers is an essential first step in the characterization of pH indicator dyes for use in the spectrophotometric pH determination. The characterization of the pH indicator dye *meta*-Cresol Purple (mCP) with a microfluidic flow spectrophotometric cell in the same temperature and salinity ranges will be reported in a companion paper. The results relayed here will therefore promote the acquisition of high quality in situ measurements of pH in polar waters and sea ice brines, and will improve the confidence in future investigations of this parameter of the carbonate system in these environments.

2. Methods

The pH of equimolal and non-equimolal Tris buffers (pH_{Tris}) in synthetic seawater and brines was determined with the electrochemical Harned cell (Bates, 1973), the only rigorous method available for the characterization of primary buffer solutions (IUPAC, 2002). The characterization was conducted in the Marine Physical Laboratory, Scripps Institution of Oceanography, University of California, San Diego, USA. The determination of the pH_{Tris} requires the determination of the standard potential of the Harned cell from e.m.f. measurements with pure HCl solutions, HCl solutions prepared in the synthetic medium, and in HCl solutions in the synthetic medium with Tris. Details of the all-glass type Harned cell, and the silver-silver chloride and hydrogen electrodes used in this study can be found in DelValls and Dickson (1998). The solutions were analysed in duplicate or triplicate at each HCl molality in the Harned cells in a thermostated water-glycol bath. The bath temperature was controlled to 0.01 °C and all e.m.f. measurements were corrected to 1 atm hydrogen gas fugacity (DelValls and Dickson, 1998). We characterized the Tris-HCl buffer in the standard equimolal Tris/Tris-H^+ composition (0.08 mol $kg_{H_2O}^{-1}$ Tris, 0.04 mol $kg_{H_2O}^{-1}$ HCl) and in a less alkaline non-equimolal Tris/Tris-H^+ composition (0.06 mol $kg_{H_2O}^{-1}$ Tris, 0.04 mol $kg_{H_2O}^{-1}$ HCl) in synthetic high ionic strength multi-electrolyte solutions matching the ionic ratios of standard seawater and seawater-derived brines. The synthetic solutions were prepared gravimetrically using the recipe in Table 1, which was based on that of standard seawater (S = 35) in DelValls and Dickson (1998). All synthetic solutions were prepared with purified salts, to maximize stability in the electrochemical response of the Harned cell. All salts (NaCl, Na_2SO_4, KCl, $CaCl_2$, $MgCl_2$) were twice re-crystallized from reagent grade salts, air-dried, annealed at 200 °C, and (except for $CaCl_2$ and $MgCl_2$) were heated to 500 °C (10 h) (Dickson, 1990a; Millero et al., 1993). The $CaCl_2$ and $MgCl_2$ salts were used to prepare approximately 1 mol $kg_{solution}^{-1}$ Ca^{2+} and Mg^{2+} working stock solutions,

Table 1
The composition and ionic strength (I) of synthetic seawater of nominal salinity 35[a].

Component	mol $kg_{H_2O}^{-1}$	mol $kg_{solution}^{-1}$
NaCl	0.42762 − m_1	0.41262
Na_2SO_4	0.02927	0.02824
KCl	0.01058	0.01021
$MgCl_2$	0.05474	0.05282
$CaCl_2$	0.01075	0.01037
[b]HCl	m_1	0
[b]Tris	m_2	0
Cl^-	0.5692	0.5492
I	0.7225	

[a] The molality (m_S, in mol $kg_{H_2O}^{-1}$) of the salts in synthetic brines of salinity S > 35 and ionic strength I_S was calculated as $m_S = m_{35} I_S/I_{35}$, with I_S = 19.9184 S/(1000–1.00198 S) (DelValls and Dickson, 1998). The concentration in mol $kg_{solution}^{-1}$ was calculated by computing the total salt mass ($\sum mass_{salt}$) and multiplying each salt molality with the factor, $1000/(1000+\sum mass_{salt})$.

[b] The molalities of HCl and Tris were chosen independent of ionic strength. In cells (B) and (C), $m_2 = 0$; in cells (D) and (E), $m_2 = 2\ m_1$ for equimolal Tris buffers.

which were used for the preparation of the synthetic media. The concentration of Ca^{2+} and Mg^{2+} in these stock solutions was determined gravimetrically with a relative standard deviation better than 0.1% by Mohr titration with 0.3 mol $kg^{-1}_{solution}$ $AgNO_3$, itself standardized similarly against purified NaCl and KCl (Dickson, 1990a; Millero et al., 1993). The working stock HCl solution (approximately 1 mol $kg^{-1}_{solution}$) was prepared gravimetrically with de-ionized water from double-distilled 6 M HCl solution. The concentration of these HCl solutions was determined by coulometry with a relative standard deviation better than 0.001%. It is standard practice to adjust the e.m.f. measurements in synthetic salt solutions so that their standard potential corresponds to that of Bates and Bower (1954). The adjustment factor is determined from e.m.f. measurements in dilute HCl solutions as described in the next section.

3. The standard potential of pure HCl solutions

The standard potential (E_o = e.m.f. at infinite proton dilution) of the cell

$$Pt;H_2(g,1atm)/HCl(m_1),De-ionized\ Water/AgCl,Ag, \quad (A)$$

was determined regularly to ensure conformity with the measurements by Bates and Bower (1954). The E_o of cell (A) was derived by solving the Nernst equation as $E_o = E + 2\,k\,\ln(\gamma_{\pm HCl}\,m_{HCl})$, where E = measured e.m.f., $\gamma_{\pm HCl}$ = mean activity coefficient of HCl, $m_{HCl} = m_1$ in cell (A), and k = RT/F, with R = gas constant = 8.31451 J mol^{-1} K^{-1}, T = absolute temperature (in K), and F = Faraday constant = 96,485.31 C mol^{-1}. The $\gamma_{\pm HCl}$ was computed as a function of ionic strength and temperature using the Pitzer parameterization. In the Pitzer formalism (Pitzer, 1973), the mean activity coefficient of HCl as an 1–1 electrolyte is calculated as $\ln\gamma_{\pm HCl} = f^{\gamma} + m_{HCl}B^{(\gamma)}_{HCl} + m^2_{HCl}C^{(\gamma)}_{HCl}$, with $f^{\gamma} = -A^{\Phi}\{[I^{0.5}/(1+bI^{0.5})] + (2/b)\ln(1+bI^{0.5})\}$, $B^{(\gamma)}_{HCl} = 2\beta^{(o)}_{HCl} + [2\beta^{(1)}_{HCl}/(\alpha^2 I)][1-(1+\alpha I^{0.5}-0.5\alpha^2 I)\exp(-\alpha I^{0.5})]$, and $C^{(\gamma)}_{HCl} = 1.5C^{(\phi)}_{HCl}$, where α = 2.0 and b = 1.2, while molality (m) and ionic strength (I) are in mol $kg_{H_2O}{}^{-1}$. The Pitzer coefficients, A^{ϕ}, $\beta^{(o)}_{HCl}$, $\beta^{(1)}_{HCl}$, and $C^{(\phi)}_{HCl}$, were all computed from the temperature functions in Millero (2009). At the HCl molality and ionic strength (both 0.010 mol $kg_{H_2O}{}^{-1}$) and temperatures used most frequently in this study for the E_o determination, $\gamma_{\pm HCl}$ = 0.9046 at 25 °C and 0.9083 at 0 °C.

The E_o determined in this study as described above ($E_o^{measured}$) and by Bates and Bower (1954) (E_o^{BB}) as computed from the temperature function in Dickson (1990b) yielded the offset $\Delta E_o^{BB} = E_o^{measured} - E_o^{BB}$. At the temperatures that $E_o^{measured}$ was determined in this study, E_o^{BB} is 0.22240 V at 25 °C, 0.23408 V at 5 °C, and 0.23659 V at 0 °C. To determine ΔE_o^{BB}, cell (A) was run on several occasions in parallel with the cells with synthetic saline and hypersaline media described in the next two sections. On average, $\Delta E_o^{BB} = -0.00012 \pm 0.00024$ V (n = 39) with m_{HCl} = 0.010 mol $kg_{H_2O}{}^{-1}$ and $\Delta E_o^{BB} = -0.00052 \pm 0.00016$ V (n = 4) with m_{HCl} = 0.005 mol $kg_{H_2O}{}^{-1}$ in cell (A) at 0, 5, and 25 °C during Harned cell runs with S = 35 synthetic seawater, while $\Delta E_o^{BB} = 0.00000 \pm 0.00005$ V (n = 37) with m_{HCl} = 0.010 mol $kg_{H_2O}{}^{-1}$ in cell (A) at 0 and 25 °C during Harned cell runs with S = 45–70 synthetic brines, and $\Delta E_o^{BB} = +0.00002 \pm 0.00005$ V (n = 17) with m_{HCl} = 0.010 mol $kg_{H_2O}{}^{-1}$ in cell (A) at 0 and 25 °C during Harned cell runs with S = 85–100 synthetic brines. To adjust the e.m.f. measurements in synthetic salt solutions so that their standard potential corresponds to that of Bates and Bower (1954), the average ΔE_o^{BB} per group of saline and hypersaline Harned cell runs was subtracted from all e.m.f. measurements in these media. The adjusted e.m.f. measurements and the ΔE_o^{BB} values used for their adjustment are reported in Table S1 in Supplementary Information for cells (B) and (C) and in Table 3 for cells (D) and (E); these cells are described in the next two sections.

4. The apparent standard potential of the Harned cell with synthetic seawater (S = 35) and synthetic brine (S > 35)

The e.m.f. measurements in the cells

$$Pt;H_2(g,1\ atm)/HCl(m_1),Synthetic\ Seawater(S=35)/AgCl,Ag \quad (B)$$

$$Pt;H_2(g,1\ atm)/HCl(m_1),Synthetic\ Brine(S>35)/AgCl,Ag \quad (C)$$

were used to determine their apparent standard potential (E_o^*) in the presence of sulphate in the synthetic solutions of this study. Sulphate ions react with protons to form bisulphate ($SO_4^{2-} + H^+ = HSO_4^-$), with a stoichiometric dissociation constant $K_{HSO_4^-} = m_{H^+}m_{SO_4^{2-}}/m_{HSO_4^-}$. In this case, instead of the free proton scale (m_{H^+}), the total proton scale has been used previously, defined as $m_{H^+}{}^T = m_{H^+} + m_{HSO_4^-} = m_{H^+}(1 + m_{SO_4^{2-}}/K_{HSO_4^-})$, with $m_{H^+}{}^T = m_{HCl} = m_1$ in cells (B) and (C) above (Campbell et al., 1993; Dickson, 1990b). Thermodynamically rigorous, the total proton scale is suitable for the determination of acidity constants (Dickson, 1990b) and, as per objective of this study, is also used here to define and determine the pH of Tris buffers in keeping with previous studies (Campbell et al., 1993; DelValls and Dickson, 1998). Conversion to the free proton scale requires knowledge of $K_{HSO_4^-}$, which is not available at below-zero temperatures. It is beyond the scope of this study to determine $K_{HSO_4^-}$ because it is not needed to determine acidity constants in the total proton scale; as outlined below, this parameter is incorporated in the determined E_o^* term of the Nernst equation for cells (B) and (C).

The E_o^* is given by re-arrangement of the Nernst equation as $E_o^* = E_o - 2\,k\,\ln\gamma_{\pm HCl} + k\,\ln(1 + m_{SO_4^{2-}}/K_{HSO_4^-}) = E + k\,\ln(m_{HCl}m_{Cl^-})$ (Campbell et al., 1993; Dickson, 1990b; Millero et al., 1993). Here, E_o, k, and $\gamma_{\pm HCl}$ are as explained in the previous section, $K_{HSO_4^-}$ and m_{HCl} as above, $m_{SO_4^{2-}}$ = total sulphate molality, m_{Cl^-} = total chloride molality, and E = measured e.m.f. in cells (B) and (C) above adjusted by ΔE_o^{BB}. The value of $E_o^* = E_o - 2k\ln\gamma_{\pm HCl} + k\ln(1 + m_{SO_4^{2-}}/K_{HSO_4^-})$ is determined at each temperature and salinity at $m_{HCl} \to 0$, the standard state of infinite dilution in the pure medium, as the intercept of the quadratic function, $E' = E + k\ln(m_{HCl}m_{Cl^-}) = a + b\,m_{HCl} + c\,m^2_{HCl}$, with $E_o^* = a$ (Campbell et al., 1993; Dickson, 1990b). The adjusted e.m.f. measurements in synthetic solutions of several different HCl molalities (n = 5–6) at each salinity and temperature (given in Table S1 in Supplementary Information) were used to obtain E′. The experimental E′ values were fitted to a quadratic function of m_{HCl} with least-squares regression in Excel (shown for S = 35 and 45 in Fig. 1) to obtain E_o^* and its standard error (equivalent to that of the intercept of the quadratic fit), which are both given in Table 2. The adjusted squared correlation coefficient of the quadratic fits ranged from 0.9421 to 0.9997 ($p < 0.00001$) and the standard error of the fits from 0.00001 to 0.00011 V. Cell (B) was investigated with m_{HCl} = 0.005–0.040 mol $kg_{H_2O}{}^{-1}$ at 25, 0, −0.6, −1.2, and −1.7 °C, the last temperature close to the freezing point of surface oceanic water [−1.93 °C, S = 35; UNESCO (1983)]. Cell (C) was investigated with m_{HCl} = 0.010–0.050 mol $kg_{H_2O}{}^{-1}$ for S = 45–100 at 25 and 0 °C, as well as the freezing point of the synthetic brine (−2.5 to −6.0 °C). The freezing point of the synthetic brines was computed from the inversion of the empirical absolute salinity-temperature (S_A-t) relationship of sea ice brines at ice-brine equilibrium, $S_A = 1000\ (1\text{–}54.11/t)^{-1}$ (Assur, 1958).

5. Determination of the pH_{Tris} in synthetic seawater (S = 35) and synthetic brines (S > 35)

The values of E_o^* in cells (B) and (C) (Table 2) were combined with e.m.f. measurements in cells (D) and (E) below, adjusted by ΔE_o^{BB} as described in the previous sections, to determine at each salinity and temperature the value of pH_{Tris} in mol $kg^{-1}_{solution}$ as $pH_{Tris} = (E - E_o^*)/(k\ln10) + \log m_{Cl^-} - \log(1 - 0.00106\,S)$ (DelValls and Dickson, 1998) (Table 3). In this equation, ln10 is the conversion factor between

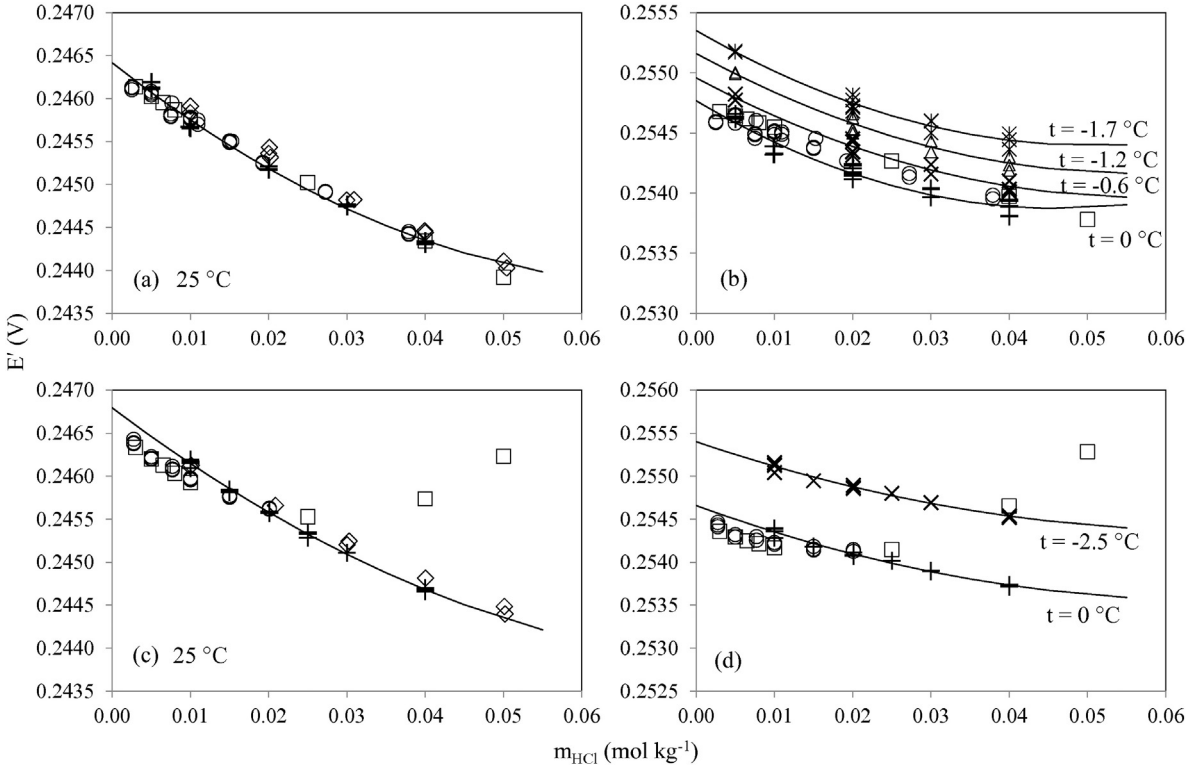

Fig. 1. The value of $E' = E + k\ln(m_{HCl}m_{Cl^-})$ versus m_{HCl} in synthetic seawater (S = 35) in panels (a) and (b), and in S = 45 synthetic seawater-based brine in panels (c) and (d). Data from previous studies are from Khoo et al. (1977) (◇), Dickson (1990b) (○), and Campbell et al. (1993) (□). The solid lines in all panels show the quadratic fit in m_{HCl} to the E′ values for the determination of E^*_o as the intercept at $m_{HCl} = 0$.

logarithmic scales and all other parameters are as before, while the last term on the right side of this equation serves to convert the pH value from mol $kg_{H_2O}^{-1}$ to mol $kg_{solution}^{-1}$.

$$\text{Pt; } H_2(g, 1\text{ atm})/HCl(m_1), Tris(m_2), \text{Synthetic Seawater}(S = 35)/AgCl, Ag \quad (D)$$

Table 2
The apparent standard potential (E^*_o) and its regression standard error (σ^*_{Eo}) (both in V) of cells (B) and (C). Values in *italics* were derived from the salinity and temperature extrapolation of Eqs. (15) and (16) in Dickson (1990b) and Eqs. (17) and (18) with the coefficients derived from the combined data sets in Campbell et al. (1993).

		this study		Dickson (1990b)	Campbell et al. (1993)
t (°C)	S	E^*_o	$\sigma^*_{E_o}$	E^*_o	E^*_o
25.0	35	0.24642	0.00005	0.24628	0.24630
0.0		0.25477	0.00004	0.25468	0.25474
−0.6		0.25496	0.00005	*0.25485*	*0.25439*
−1.2		0.25516	0.00006	*0.25502*	*0.25458*
−1.7		0.25535	0.00006	*0.25518*	*0.25475*
25.0	45	0.24680	0.00003	0.24651	0.24655
0.0		0.25466	0.00004	0.25442	0.25448
−2.5		0.25540	0.00004	*0.25515*	*0.25470*
25.0	50	0.24664	0.00008	*0.24641*	*0.24582*
0.0		0.25428	0.00009	*0.25411*	*0.25358*
−2.8		0.25511	0.00009	*0.25491*	*0.25447*
25.0	60	0.24637	0.00006	*0.24579*	*0.24516*
0.0		0.25363	0.00006	*0.25314*	*0.25259*
−3.4		0.25461	0.00006	*0.25405*	*0.25364*
25.0	70	0.24578	0.00002	*0.24462*	*0.24399*
0.0		0.25277	0.00008	*0.25166*	*0.25114*
−4.0		0.25391	0.00009	*0.25268*	*0.25235*
25.0	85	0.24519	0.00013	*0.24180*	*0.24122*
0.0		0.25177	0.00004	*0.24846*	*0.24805*
−5.0		0.25311	0.00004	*0.24962*	*0.24949*
25.0	100	0.24381	0.00012	*0.23756*	*0.23713*
0.0		0.24989	0.00006	*0.24388*	*0.24368*
−6.0		0.25142	0.00006	*0.24515*	*0.24536*

$$\text{Pt; } H_2(g, 1\text{ atm})/HCl(m_1), Tris(m_2), \text{Synthetic Brine}(S>35)/AgCl, Ag \quad (E)$$

With $[\text{Tris-H}^+] = m_1$ and $[\text{Tris}] = m_2 - m_1$ in cells (D) and (E) above, at stoichiometric equilibrium, the reaction, Tris + HCl = Tris-$H^+ + Cl^-$, leads to equimolal Tris and Tris-H^+ molalities in cell solutions containing $m_1 = 0.04$ mol $kg_{H_2O}^{-1}$ HCl and $m_2 = 0.08$ mol $kg_{H_2O}^{-1}$ Tris. Because the equimolal pH_{Tris} is alkaline at low temperatures ($pH_{Tris} \approx 9$), a less alkaline, non-equimolal Tris buffer was also characterized with the Harned cell protocol with $m_1 = 0.04$ mol $kg_{H_2O}^{-1}$ and $m_2 = 0.06$ mol $kg_{H_2O}^{-1}$, yielding a molality ratio, $R_{Tris} = m_{Tris}/m_{Tris-H^+} = 0.5$. To examine the internal consistency of the e.m.f. measurements in these non-equimolal Tris-HCl buffers, their pH was also computed from the equimolal pH_{Tris}, when available, and their R_{Tris} using the Henderson – Hasselbalch equation (Pratt, 2014), $pH_{Tris} = pK^*_{Tris} + \log R_{Tris}$, which is derived from the stoichiometric equilibrium of the Tris-H^+ dissociation reaction (Millero, 2009), with pK^*_{Tris} equivalent to the equimolal pH_{Tris} when $R_{Tris} = 1$.

The E^*_o and pH_{Tris} data from this study alone and combined with relevant data at above-zero temperatures from earlier studies were fitted to non-linear equations of temperature and salinity or ionic strength using the Regression function in the Data Analysis Tool of Excel. The fitted coefficients of these equations, along with the adjusted squared correlation coefficient (r^2) and the standard error of the fit (σ_{fit}), as well as the number of fitted observations (n), are all reported from the Regression output in subsequent sections. Information about the standard error of the individual fitted coefficients is reported in Tables S2 and S3 in Supplementary Information.

6. Results

The focus of this study was the characterization of the pH of Tris buffers at below-zero temperatures but e.m.f. measurements were also obtained at 25 and 0 °C for evaluation relative to the existing datasets at overlapping temperature and salinity ranges. We kept this

Table 3
The potential (E_{Tris}, in V) of cells (D) and (E) with Tris buffer solutions in synthetic seawater and brines. The E_{Tris} is the value after adjustment by ΔE_o^{BB} (in V) so that the standard potential of the cells corresponds to that of Bates and Bower (1954) [see *Methods* and DelValls and Dickson (1998) for details]. The concentrations of the Tris species (m_{Tris}, m_{Tris-H^+}) and total chloride (m_{Cl^-}) in solution are in mol $kg_{H_2O}^{-1}$, while the pH_{Tris} is the negative common logarithm of the proton concentration in mol $kg_{solution}^{-1}$ on the total proton scale.

S	t (°C)	m_{Tris}	m_{Tris-H^+}	m_{Cl^-}	ΔE_o^{BB}	E_{Tris}			pH_{Tris}		
35	24.996	0.04	0.04	0.56918	−0.00012	0.73863	0.73873	0.73870	8.092	8.094	8.093
	0.004					0.75129	0.75136	0.75134	8.933	8.934	8.934
	−0.001					0.75130	0.75137	0.75134	8.933	8.934	8.934
	−0.619					0.75158	0.75164	0.75163	8.955	8.957	8.956
	−1.165					0.75170	0.75190	0.75187	8.972	8.976	8.975
	−1.712					0.75205	0.75216	0.75214	8.994	8.996	8.996
45	25.000			0.73949	0.00000	0.73317	0.73320		8.111	8.112	
	−0.003					0.74633	0.74628		8.962	8.961	
	−2.499					0.74755	0.74751		9.054	9.054	
50	24.996			0.82602	0.00000	0.73080	0.73080		8.125	8.125	
	−0.002					0.74421	0.74418		8.980	8.980	
	−2.795					0.74561	0.74558		9.084	9.084	
60	24.997			1.00190	0.00000	0.72655	0.72659		8.146	8.147	
	−0.006					0.74024	0.74037		9.008	9.010	
	−3.422					0.74202	0.74215		9.137	9.139	
70	24.998			1.18141	0.00000	0.72280	0.72284		8.169	8.170	
	−0.002					0.73690	0.73693		9.038	9.039	
	−3.999					0.73904	0.73908		9.190	9.191	
35	0.003	0.02	0.04	0.56918	+0.00002	0.73511	0.73505	0.73506	8.634	8.633	8.633
45	0.002			0.73949	+0.00002	0.73019	0.73013	0.73012	8.664	8.663	8.663
50	24.996			0.82599	0.00000	0.71299	0.71300		7.824	7.824	
	−0.002					0.72782	0.72779		8.678	8.677	
	−2.795					0.72939	0.72937		8.782	8.781	
60	24.997	0.02	0.04	1.00163	0.00000	0.70879	0.70876		7.846	7.845	
	−0.006					0.72399	0.72402		8.708	8.708	
	−3.422					0.72598	0.72600		8.837	8.837	
70	24.998			1.18130	0.00000	0.70504	0.70504		7.869	7.869	
	−0.002					0.72053	0.72052		8.736	8.736	
	−3.999					0.72291	0.72290		8.888	8.888	
85	24.996			1.45800	+0.00002	0.70046	0.70046	0.70043	7.900	7.900	7.900
	24.999					0.70049	0.70024	0.70025	7.901	7.897	7.897
	0.000					0.71642			8.778		
	−0.001					0.71660	0.71650	0.71650	8.781	8.779	8.779
	−5.001					0.71950			8.970		
	−5.000					0.71968	0.71960	0.71961	8.974	8.972	8.972
100	25.000			1.74393	+0.00002	0.69605	0.69573	0.69567	7.935	7.929	7.928
	0.001					0.71264	0.71261	0.71261	8.828	8.827	8.827
	−6.001					0.71643	0.71643	0.71641	9.063	9.063	9.062

protocol throughout the experimental salinity range (35–100) and report the results at 25 and 0 °C here in order to provide data useful for occasions in sea ice studies when pH measurement at sub-zero temperatures is not possible due to harsh field conditions and restrictions by equipment or method.

6.1. The standard potential of the Harned cell to the freezing point of synthetic seawater and brines

The E_o^* values at each experimental temperature and salinity along with their standard error are given in Table 2 and are shown in Fig. 2. The e.m.f. measurements at S = 35 (Fig. 1a,b) were consistent with published data at 25 and 0 °C (Campbell et al., 1993; Dickson, 1990b; Khoo et al., 1977), while those made at S = 45 (Fig. 1c,d) were consistent with the values in Khoo et al. (1977) at 25 °C. The current E_o^* values at 25 and 0 °C and S = 35 and 45 were different by <+0.00030 V from previous determinations in these conditions (Campbell et al., 1993; Dickson, 1990b). No other direct comparison is possible as the remainder of the current data extend beyond the temperature minimum and salinity maximum of the previous data sets. An indirect comparison can be made using the extrapolation of the ionic strength and temperature function of E_o^* in Dickson (1990b) and in Campbell et al. (1993). This will also allow a direct evaluation of the extrapolation as practiced by necessity so far by sea ice scientists.

The current E_o^* values at below-zero temperatures and S = 35 were +0.00010 to +0.00020 V and +0.00060 V different from those predicted by extrapolation of the equations in Dickson (1990b) and Campbell et al. (1993), respectively (Table 2). These differences are equivalent to 0.002–0.011 pH unit for the Tris buffer in synthetic seawater. A revised non-linear function of temperature is given below for E_o^* in synthetic seawater (S = 35) from the regression fit to the combined past and current data from 55 to −1.7 °C ($r^2 = 0.99995$, $p < 0.00001$, $n = 27$, $\sigma_{fit} = 0.00004$ V; the fitted residuals are shown in Fig. S1a in Supplementary Information), with E_o = the Bates and Bower (1954) standard potential of the Harned cell as fitted by Dickson (1990b) and T = temperature (in K):

$$E_o^* - E_o = 0.583228 - 1.5914057 \times 10^{-2} T + 2.5229012 \times 10^{-3} T \ln T - 1.12824 \times 10^{-6} T^2, \quad (1)$$

The difference between the current E_o^* values in the synthetic brines (S ≥ 45) and the extrapolated values from the existing equations (Table 2) ranged from +0.00020 to +0.00670 V (equivalent to 0.003–0.118 pH unit), increasing with increasing salinity throughout the experimental temperature range (Fig. 2). The current measurements provide for a more accurate and reliable measurement of the pH in ice-brine systems. To facilitate this application, we combined the E_o^* value at the freezing point of seawater derived from Eq. (1) above (E_o^* = 0.25540 V at −1.93 °C and S = 35 at 1 atm total pressure) with the values obtained at the different freezing points of S ≥ 45 brines (Table 2) to obtain a best-fit temperature function of E_o^* applicable to thermally equilibrated sea ice brines. We found E_o^* to be best described ($r^2 = 0.98906$, $p = 0.00005$, $n = 7$, $\sigma_{fit} = 0.00015$ V; the fitted residuals are shown in Fig. S1b in

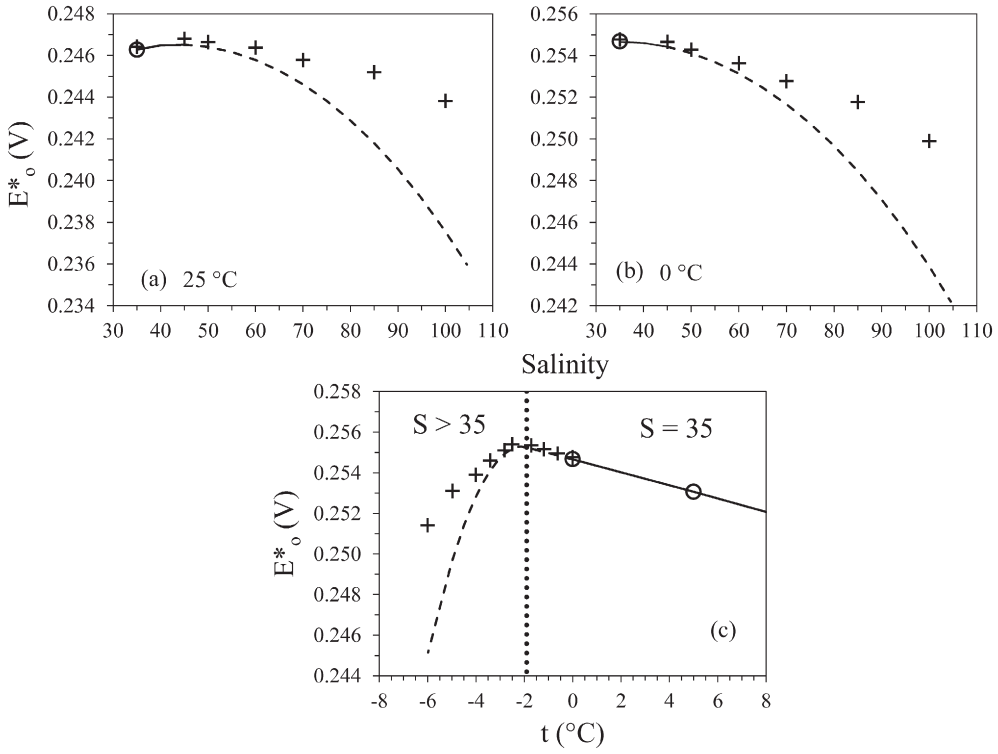

Fig. 2. The apparent standard potential of the Harned cell with synthetic seawater and synthetic seawater-based brine as a function of salinity in panels (a) and (b), and as a function of temperature in panel (c). Open circles represent experimental data from Dickson (1990b). The solid line represents the best-fit Eq. (16) of Dickson (1990b) within its experimental ionic strength and temperature ranges, while the dashed line represents its extrapolation to S > 45 and below-zero temperatures. In panel (c), the temperatures below the freezing point of S = 35 seawater (−1.93 °C; dotted vertical line) represent the freezing points at S > 35 salinities.

Supplementary Information) by a quadratic function of temperature (T, in K) at the freezing point of seawater and seawater-derived brines from −1.93 to −6.00 °C (S = 35–100):

$$E_o^* = -11.632112 + 8.7319058 \times 10^{-2}T - 1.60345606 \times 10^{-4}T^2, \quad (2)$$

An extended equation is provided below for the computation of E_o^* by interpolation at any salinity and temperature outside the restricted conditions of Eqs. (1) and (2) above but within the limits of the experimental range. The interpolation will be useful for the characterization of pH buffers (on the total proton scale) on such occasions. Although the current E_o^* data set is sparse as a function of temperature, it was combined with the data sets in Dickson (1990b) and Campbell et al. (1993) for an overall best fit ($r^2 = 0.99186$, $p < 0.00001$, $n = 133$, $\sigma_{fit} = 0.00008$ V) in the function format of the previous studies in ionic strength (I, in molality) and temperature (T, in K), with E_o from Dickson (1990b) as before:

$$\begin{aligned} E_o^* - E_o = {} & (0.8416344 - 2.0574375 \times 10^{-2}T + 3.1544753 \times 10^{-3}T\ \ln T \\ & - 2.6635 \times 10^{-8}T^2)I^{0.5} + (-0.3356577 + 7.581873 \times 10^{-3}T \\ & - 1.1680967 \times 10^{-3}T\ \ln T)I + (1.1146 \times 10^{-2} \\ & + 4.525 \times 10^{-5}T)I^{1.5} - 4.67174 \times 10^{-3}I^2, \end{aligned} \quad (3)$$

In the above equation, the ionic strength was calculated as a function of salinity as described in Table 1, while the fitted residuals are shown in Fig. 3. Eq. (3) is valid at temperatures (*i*) between 0 and 55 °C for I < 0.7225 m (S < 35), (*ii*) between the freezing point and 55 °C for 0.7225 m ≤ I ≤ 0.9387 m (35 ≤ S ≤ 45), and (*iii*) between the freezing point and 25 °C for 0.9387 m < I ≤ 2.2136 m (45 < S ≤ 100). At 25 °C

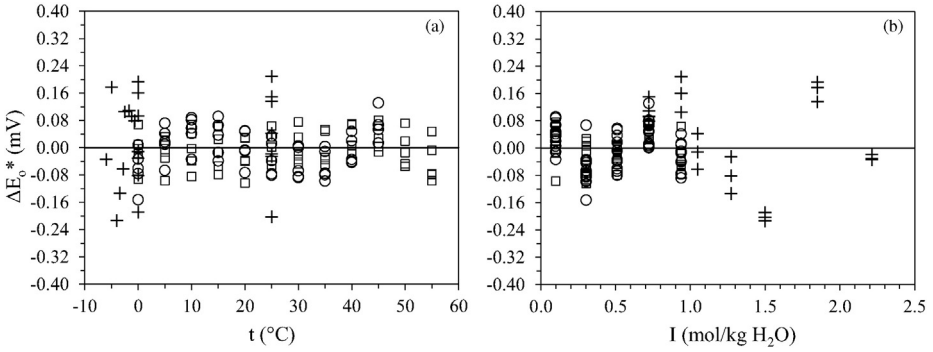

Fig. 3. Residuals in E_o^* as a function of (a) temperature and (b) ionic strength (molal). The residuals are between the experimental values and the fitted values from Eq. (3). The experimental values are from Table 2 in this study (+), from Table 3 in Dickson (1990b) (○), and from Table 3 in Campbell et al. (1993) (□).

and I = 0.7225 m, Eq. (3) yields E^*_o = 0.24627 V, while at −6 °C and I = 2.2136 m, E^*_o = 0.25145 V (see Table 2 for observed values).

6.2. The pH of Tris buffers to the freezing point of synthetic seawater and brines

The pH values of the equimolal Tris buffer are listed in Table 3 and are shown in Fig. 4. The equimolal pH_{Tris} in synthetic seawater at 25 °C and 0 °C from the observed E^*_o (Table 2) and the e.m.f. measurements in cells (D) and (E) (Table 3) was within 0.002 pH unit from the values computed from the salinity and temperature function in DelValls and Dickson (1998) based on their experimental measurements at S = 20–40 and 0–45 °C. The equimolal pH_{Tris} in synthetic seawater at sub-zero temperatures differed by 0.000–0.004 pH unit from the values obtained from the extrapolated DelValls and Dickson (1998) equation. The best-fit temperature (T, in K) function based on the combined current and previous data sets from 45 °C to the freezing point of S = 35 seawater (r^2 = 0.999997, p < 0.00001, n = 121, σ_{fit} = 0.001 pH unit; the fitted residuals are shown in Fig. S2a in Supplementary Information) is given by the following equation:

$$pH_{Tris}(\text{equimolal}) = -322.08663 + 10570.47\ T^{-1} - 1.0408523 \times 10^{-1} T + 57.17485\ \ln T, \quad (4)$$

The equimolal pH_{Tris} in synthetic brines (S ≥ 45) was determined up to S = 70. It was within 0.007 pH unit at S = 45 and 50 from the values predicted from the extrapolation of the DelValls and Dickson (1998) function but was lower than the extrapolated values by 0.009–0.019 and 0.021–0.036 pH unit at S = 60 and 70, respectively, at all examined temperatures, suggesting increasingly unsuitable values from extrapolation at high salinities regardless of temperature (Fig. 4). Combining the value of the equimolal pH_{Tris} at the freezing point of S = 35 seawater from Eq. (4) above (equimolal pH_{Tris} = 9.0039 at −1.93 °C) with the observations obtained at the different freezing points of S ≥ 45 brines (Table 3), the equimolal pH_{Tris} at ice-brine thermal equilibrium was found to be best described (r^2 = 0.99929, n = 9, p < 0.00001, σ_{fit} = 0.002 pH unit; the fitted residuals are shown in Fig. S2b in Supplementary Information) to −4 °C and S = 70 by the following function of temperature (T, in K):

$$pH_{Tris}(\text{equimolal}) = -300435.6052 + 7240100.99\ T^{-1} - 99.5850583\ T + 53678.964954\ \ln T, \quad (5)$$

The non-equimolal $pH_{R_{Tris}=0.5}$ values are given in Table 3 and are shown in Fig. 4. On the occasions when both the equimolal and the non-equimolal buffers were measured (35 ≤ S ≤ 70), the non-equimolal $pH_{R_{Tris}=0.5}$ values were within 0.001 pH unit from those determined from the Henderson – Hasselbalch equation described in the earlier section *Determination of the pH_{Tris} in synthetic seawater (S = 35) and synthetic brines (S > 35)*. The $pH_{R_{Tris}=0.5}$ at the freezing point was determined for 50 ≤ S ≤ 100 and −6.0 °C ≤ t ≤ −2.8 °C. The best-fit function of temperature (T, in K) for the non-equimolal $pH_{R_{Tris}=0.5}$ in the temperature and salinity conditions of thermally equilibrated seawater-derived brines is as follows (r^2 = 0.99991, n = 13, p < 0.00001, σ_{fit} = 0.001 pH unit; the fitted residuals are shown in Fig. S2c in Supplementary Information):

$$pH_{R_{Tris}=0.5} = -725997.4416 + 17447191.73\ T^{-1} - 241.432111\ T + 129781.87456\ \ln T, \quad (6)$$

As mentioned at the beginning of the *Results* section, there can be occasions when the measurement of pH in cold media, such as sea ice brines, may not be possible at below-zero temperature. To provide interpolation power for these occasions, the data sets of the equimolal

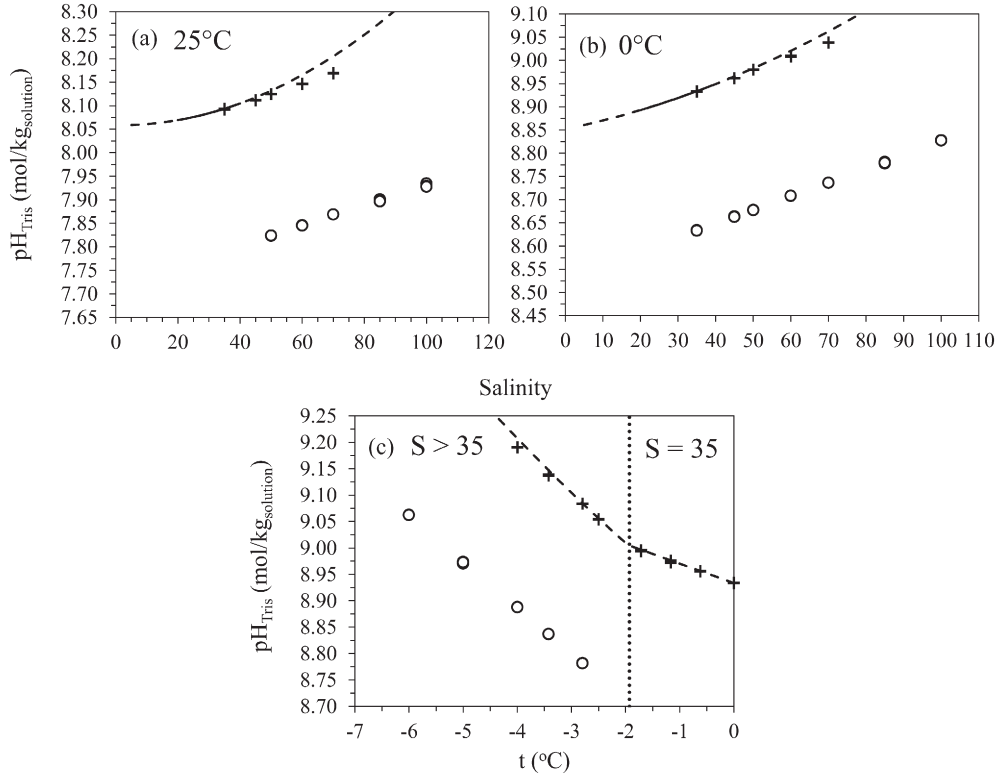

Fig. 4. The pH of Tris buffer solutions (on the total proton scale) in synthetic seawater and synthetic brine as a function of salinity in panels (a) and (b), and as a function of temperature at sub-zero temperatures in panel (c). The observations from this study are from the equimolal Tris buffer (+) (molality ratio, $R_{Tris} = m_{Tris}/m_{Tris-H^+} = 1$) and the non-equimolal Tris buffer (○) (R_{Tris} = 0.5). The solid line represents the best-fit Eq. (18) of DelValls and Dickson (1998) within its experimental salinity and temperature ranges, while the dashed line represents its extrapolation to S < 20 and S > 40, and below-zero temperatures. In panel (c), the temperatures below the freezing point of S = 35 seawater (−1.93 °C; dotted vertical line) represent the freezing points at S > 35 salinities.

pH_{Tris} from this study and the study of DelValls and Dickson (1998) were combined to obtain a best fit in the format of the latter study, valid at temperatures (*i*) between 0 and 45 °C for S < 35, (*ii*) between the freezing point and 45 °C for 35 ≤ S < 45, and (*iii*) between the freezing point and 25 °C for 45 ≤ S ≤ 70. The best fit equation in salinity (S) and temperature (T, in K) ($r^2 = 0.999995$, $n = 273$, $p < 0.00001$, $\sigma_{fit} = 0.001$ pH unit; the fitted residuals are shown in Fig. 5a, c) is

$$\begin{aligned} pH_{Tris}(\text{equimolal}) = {} & 536.08338 - 54.732367\,S + 0.8518518\,S^2 \\ & + (0.1675218 - 1.72224095 \times 10^{-2}\,S \\ & + 2.66720246 \times 10^{-4}\,S^2)\,T + (-10873.5234 \\ & + 1369.56485\,S - 21.34442\,S^2)\,T^{-1} \\ & + (-95.04342 + 9.7014355\,S \\ & - 0.1509014\,S^2)\,\ln T, \end{aligned} \quad (7)$$

At 25 °C and S = 35, Eq. (7) yields pH_{Tris} (equimolal) = 8.094, while at −4 °C and S = 70, pH_{Tris} (equimolal) = 9.191 (see Table 3 for observed values). The equivalent overall fit on the current limited non-equimolal $pH_{R_{Tris}=0.5}$ data set yielded the following function of salinity and temperature (T, in K) at 50 ≤ S ≤ 100 and from the freezing point of such brines to 25 °C ($r^2 = 0.99999$, $n = 41$, $p < 0.00001$, $\sigma_{fit} = 0.002$ pH unit; the fitted residuals are shown in Fig. 5b, d):

$$\begin{aligned} pH_{R_{Tris}=0.5} = {} & 144.4361 - 1.0809685\,S + 6.023772 \times 10^{-3}\,S^2 \\ & + \left(6.18411 \times 10^{-2} - 8.17397 \times 10^{-4}\,S + 4.27187 \times 10^{-6}\,S^2\right)T \\ & + (-27.233738 + 0.2329236\,S - 1.281138 \times 10^{-3}\,S^2)\,\ln T, \end{aligned} \quad (8)$$

Using Eq. (8) above, the predicted $pH_{R_{Tris}=0.5} = 8.637$ at 0 °C and S = 35, and $pH_{R_{Tris}=0.5} = 8.664$ at 0 °C and S = 45. These values were within 0.004 pH unit from the measured values (Table 3), and so it is reliable to extend Eq. (8) to these salinities.

7. Discussion

The investigation of the carbonate system in oceanic waters and the determination of the potential for air-sea CO_2 exchange have intensified in an attempt to understand the implications on global climate of the increase in the atmospheric CO_2 since the industrial revolution. The required sampling and analytical protocols have been improved through continual method and instrument development, allowing dense sampling in space and time for any pair of the 4 measurable parameters of the carbonate system (TA, DIC, pH, fCO_2) (DOE, 1994; Hales et al., 2004; Liu et al., 2011). While the measurement of all 4 parameters is now routine in open ocean waters (e.g., Millero et al., 2002), including polar waters (Bates and Mathis, 2009; Bates et al., 2006), the same is not true for oceanic environments at sub-zero temperatures, such as sea ice. At the salinity and temperature conditions in sea ice brines, the concentrations of TA and DIC, as well as fCO_2 naturally cover large ranges controlled by the physical concentration of seawater solutes during the freezing of seawater and further cooling of internal sea ice brines, dilution of brine solutes by meltwater during sea ice melt, biological activity, $CaCO_3$ precipitation and dissolution, and CO_2 gas exchange (Delille et al., 2007; Dieckmann et al., 2008; Gleitz et al., 1995; Miller et al., 2011a, 2011b; Munro et al., 2010; Papadimitriou et al., 2012; Papadimitriou et al., 2007; Papadimitriou et al., 2004). By extension, large variations in brine pH can also be expected in such environments, but there is only rudimentary knowledge of pH changes in sea ice as direct determination of this parameter has been hampered by lack of characterized calibration standards (buffers, indicator dyes) and unsuitable analytical set-ups for the sub-zero temperatures and, in the case of internal sea ice brines, highly saline conditions (S > 35).

Currently, the pH measurement protocols in sea ice and sub-zero temperature oceanic waters, restricted by the temperature limitation of both buffers and technique, have only been capable of pH measurements at (constant) above-zero temperature. For example, Delille et al. (2007) used commercial glass electrodes and high salinity Tris and Aminopyridine buffers for instrument calibration on samples returned

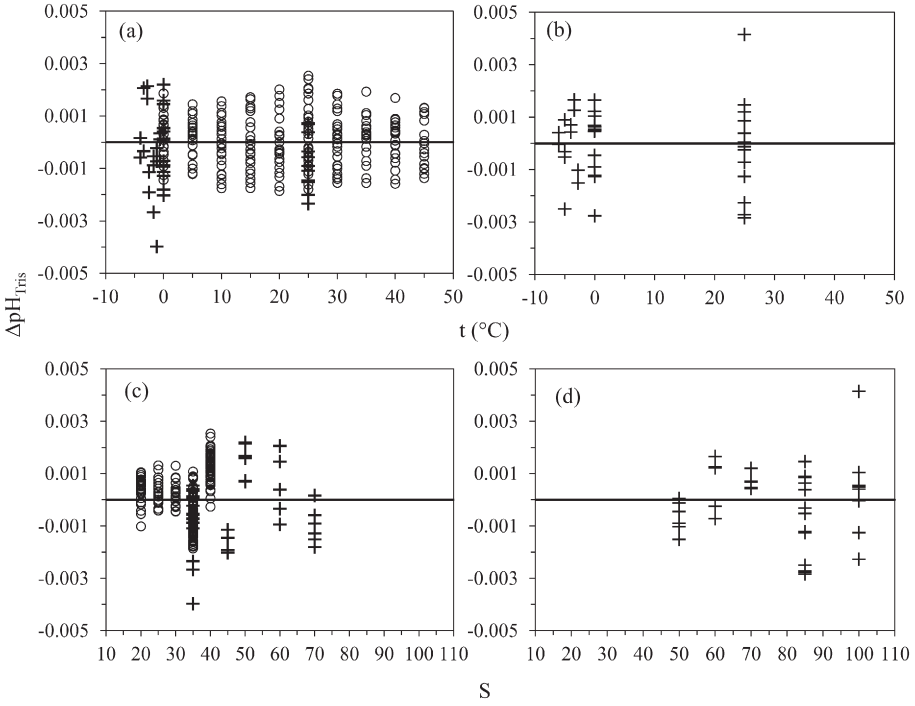

Fig. 5. Residuals in pH_{Tris} (in mol $kg^{-1}_{solution}$ on the total proton scale) as a function of temperature in panels (a) and (b), and as a function of salinity in panels (c) and (d). The residuals are between the experimental values and the fitted values from Eq. (7) for the equimolal Tris buffer (molality ratio, $R_{Tris} = m_{Tris}/m_{Tris-H^+} = 1$) in panels (a) and (c), and between the experimental values and the fitted values from Eq. (8) for the non-equimolal Tris buffer ($R_{Tris} = 0.5$) in panels (b) and (d). The experimental values are from Table 3 in this study (+) and as computed from the results for the $m_{Tris} = m_{Tris\text{-}H^+} = 0.04$ mol kg^{-1} buffer in Table 2 of DelValls and Dickson (1998) (○).

to the laboratory and maintained at 1–3 °C, and so did Gleitz et al. (1995) at 20–22 °C using NBS standard buffers. Miller et al. (2011a) used the spectrophotometric technique with un-purified mCP as the pH-sensitive indicator dye at 25 °C, as did Hare et al. (2013) at 0 °C. A technique based on the pH-sensitive fluorescence properties of acridine and harmine has been developed and applied to fresh and salty ice surfaces, but solely for monitoring rather than quantification of pH, due to lack of suitable characterization and calibration of the fluorescence properties of these probes (Wren and Donaldson, 2012).

In this study, we electrochemically characterized the pH_T (total proton scale) of Tris-HCl buffers using the Harned cell, the only rigorous method available for the task (IUPAC, 2002). Use of these buffers can facilitate the calibration of the analytical pH instrumentation at the experimental temperature and salinity ranges of this study. The pH_T of the Tris-HCl buffers was increasingly alkaline with increasing salinity at constant temperature and with decreasing temperature at constant salinity (Table 3; Fig. 4). The equimolal Tris buffer covered a pH_T range from 8.09 at S = 35 and 25 °C to 9.19 at the freezing point of an S = 70 synthetic brine (−4 °C) (Table 3). The pH_T of the non-equimolal ($R_{Tris} = 0.5$) Tris buffer ranged from 8.63 at S = 35 and 0 °C to 9.06 at the freezing point of an S = 100 synthetic brine (−6 °C) (Table 3) and was 0.3 pH unit less alkaline than its equimolal counterpart (Fig. 4) as predicted using the stoichiometric Tris-HCl equilibrium and the Henderson-Hasselbalch equation. On the strength of this evidence and the study of Pratt (2014) in synthetic seawater, Tris-HCl buffers of varying R_{Tris} and, hence, pH_T can be prepared if needed with the protocol outlined in *Methods*, and their pH_T can be estimated reliably with the Henderson-Hasselbalch equation and the data presented here for investigations within the temperature and salinity ranges of this study.

The pH_T ranges for the equimolal and non-equimolal ($R_{Tris} = 0.5$) Tris buffers covered the alkaline spectrum of pH estimates at in-situ (below-zero) temperatures in sea ice. Delille et al. (2007) reported pH_T values ranging from 8.4 to 9.4 in Antarctic fast ice brines (S = 24–89). In sackhole brines from the Weddell Sea, Antarctica, Papadimitriou et al. (2007) determined a pH_{SWS} (seawater proton scale) range of 8.4 to 8.8, while Gleitz et al. (1995) reported a pH_{SWS} range of 7.8 to 9.9. Hare et al. (2013) reported pH_T values between 7.1 and 9.5 in frost flowers, bulk ice cores, and brines from artificial sea ice grown at an outdoors experimental facility. In the Arctic Ocean, pH_T ranged from 7.7 to 12.1 in frost flowers and sea ice brines (Fransson et al., 2013), and from 8.3 to 8.5 (free proton scale, pH_F) in sackhole brines (S = 68–163) (Miller et al., 2011a) in the Amundsen Gulf, while Rysgaard et al. (2012) reported pH_T values between 9.9 and 10.1 in sea ice meltwater. In all these previous field studies, the pH values at in situ (below-zero) temperatures have been computed from measured TA and DIC in sea ice environments (Brown et al., 2014; Papadimitriou et al., 2009; Papadimitriou et al., 2007) or from the pH measured directly in the sea ice medium at above-zero temperatures and either TA or DIC (Brown et al., 2014; Delille et al., 2007; Fransson et al., 2013; Gleitz et al., 1995; Hare et al., 2013; Miller et al., 2011a). In those instances, the pH at in situ (below-zero) temperatures has been derived by solving the system of equations that describe the thermodynamic relationships of the marine carbonate system (DOE, 1994) but with the caveat that the relevant equilibrium constants have not yet been characterized at sub-zero temperatures. Therefore, the use of this approach and the derived pH at the in situ (below-zero) temperatures rely on extrapolation of the existing oceanographic salinity and temperature functions of the equilibrium constants with discouragingly large uncertainties (Brown et al., 2014).

The electrochemical characterization of the Tris buffer system in this study enables the spectrophotometric characterization of pH indicator dyes in seawater-based hypersaline media at below-zero temperatures. Both techniques and their results will free the sea ice biogeochemical community from the uncertainty in the measurement of pH in sea ice by affording investigators direct pH determination in sea ice brines down to −6 °C and salinity 100. Sea ice has been found to become impermeable at a porosity <5% (as relative brine volume), coincident with a sea ice temperature of −5 °C at a bulk sea ice salinity of 5 (Cox and Weeks, 1975; Golden et al., 1998), or colder in more saline bulk sea ice, and vice versa, based on the phase relationships in the medium (Cox and Weeks, 1983). Hence, sea ice in the current experimental temperature range ($-2 \le t \le -6$ °C) is permeable to material transport via the brine channels. As a result, the current experimental conditions are pertinent to the study of the exchange potential of the brine carbonate system in sea ice with the underlying ocean and the atmosphere above.

Major compositional changes in the internal brine in sea ice will occur at temperatures well below −6 °C as a result of extensive precipitation of hydrated salts, such as mirabilite, gypsum, and hydrohalite (Butler et al., 2016; Butler and Kennedy, 2015; Marion, 2001). Consequently, a different logistical approach is required for the study of the brine carbonate system in the coldest compositional spectrum in sea ice, which is nearest to the atmosphere. Further work below the minimum temperature presented here must take into account mineral dynamics in sea ice for the determination of the chemical composition of the internal brines, which will inform the composition of synthetic or natural solutions to be used in the laboratory for the characterization of pH buffers and indicator dyes.

8. Conclusions

The current data set established explicitly the value of one of the important parameters in the study of the carbonate system, the pH of the Tris-HCl buffer system, in sub-zero temperature saline environments and within international standards. The pH of the Tris buffer was fully characterized on the total proton scale in the temperature range from 25 °C to the freezing point of S = 35 seawater (freezing point: −1.93 °C) and seawater-derived brines up to a salinity of 100 (freezing point: −6.0 °C). The difference between measurements at sub-zero temperatures and the extrapolated values computed from the existing above-zero temperature data sets may be negligible at S = 35 in terms of both the apparent standard potential of the electrochemical Harned cell and the equimolal pH_{Tris} but increased systematically with increasing salinity at all temperatures. Based on the apparent standard potential of the Harned cell, this discrepancy was found to be equivalent to 0.118 pH unit at the highest salinity investigated here (S = 100), a substantial deviation with consequent discrepancies in other parameters of the carbonate system derived from it relying on extrapolation of existing electrochemical and oceanographic data sets defined for above-zero temperatures and S = 0–50. Hence, the current data will provide considerable improvement in the study of pH in cold saline and hypersaline conditions relative to the only choice of extrapolation available until now to biogeochemists. For a more complete characterization of the carbonate system in the cryosphere, the dissociation constants of its weak acids and bases (e.g., carbonic and boric acids) must be determined at below-zero temperatures.

Acknowledgements

We thank Makaila Lashomb for training S. Papadimitriou in the Harned cell protocol, Britain Richardson for running the Harned cell at the highest salinities, Guy Emanuele for his laboratory support, and George Anderson for providing the coulometric measurements and the tickets for the La Jolla Symphony & Chorus concerts. We also thank two anonymous reviewers for their helpful comments. The work was supported by NERC grant NE/J011096/1.

Appendix A. Supplementary data

Supplementary data to this article can be found online at http://dx.doi.org/10.1016/j.marchem.2016.06.002.

References

Arrigo, K.R., Worthen, D.L., Lizotte, M.P., Dixon, P., Dieckmann, G.S., 1997. Primary production in Antarctic sea ice. Science 276, 394–397.

Assur, A., 1958. Composition of Sea Ice and its Tensile Strength in Arctic Sea Ice. Vol. 598. U. S. National Academy of Sciences, National Research Council, Publ, pp. 106–138.

Bates, R.G., 1973. Determination of pH: Theory and Practice. Wiley, New York.

Bates, R.G., Bower, V.E., 1954. Standard potential of the silver-silver-chloride electrode from 0° to 95 °C and the thermodynamic properties of dilute hydrochloric acid solutions. J. Res. Natl. Bur. Stand. (US) 53, 283–290.

Bates, N.R., Mathis, J.T., 2009. The Arctic Ocean marine carbon cycle: evaluation of air-sea CO_2 exchanges, ocean acidification impacts and potential feedbacks. Biogeosciences 6, 2433–2459.

Bates, N.R., Moran, S.B., Hansell, D.A., Mathis, J.T., 2006. An increasing CO_2 sink in the Arctic Ocean due to sea-ice loss. Geophys. Res. Lett. 33 (1–77), 2006.

Brown, K.A., Miller, L.A., Davelaar, M., Francois, R., Tortell, P.D., 2014. Over-determination of the carbonate system in natural sea-ice brine and assessment of carbonic acid dissociation constants under low temperature, high salinity conditions. Mar. Chem. 165, 36–45.

Butler, B.M., Kennedy, H., 2015. An investigation of mineral dynamics in frozen seawater brines by direct measurement with synchrotron X-ray powder diffraction. J. Geophys. Res. Oceans 120, 5686–5697 http://dx.doi.org/10.1002/2015JC011032.

Butler, B.M., Papadimitriou, S., Santoro, A., Kennedy, H., 2016. Mirabilite solubility in equilibrium sea ice brines. Geochim. Cosmochim. Acta 182, 40–54.

Campbell, D.M., Millero, F.J., Roy, R., Roy, L., Lawson, M., Vogel, K.M., Moore, C.P., 1993. The standard potential for the hydrogen-silver, silver chloride electrode in synthetic seawater. Mar. Chem. 44, 221–233.

Chierici, M., Fransson, A., 2009. Calcium carbonate saturation in the surface water of the Arctic Ocean: undersaturation in freshwater influenced shelves. Biogeosciences 6, 2421–2431.

Cox, G.F.N., Weeks, W.F., 1975. Brine drainage and initial salt entrapment in sodium chloride ice. CRREL Research Report 345.

Cox, G.F.N., Weeks, W.F., 1983. Equations for determining the gas and brine volumes in sea ice samples. J. Glaciol. 29, 306–316.

Delille, B., Jourdain, B., Borges, A.V., Tison, J.-L., Delille, D., 2007. Biogas (CO_2, O_2, dimethylsulfide) dynamics in spring Antarctic fast ice. Limnol. Oceanogr. 52, 1367–1379.

DelValls, T.A., Dickson, A.G., 1998. The pH of buffers based on 2-amino-2 hydroxymethyl-1,3-propanediol ('tris') in synthetic seawater. Deep-Sea Res. 45, 1541–1554.

Deming, J.W., 2010. Sea ice bacteria and viruses. In: Thomas, D.N., Dieckmann, G.S. (Eds.), Sea Ice, second ed. Wiley-Blackwell, Oxford, pp. 247–282.

Dickson, A.G., 1990a. The thermodynamics of the dissociation of boric acid in synthetic seawater from 273.13 to 318.15 K. Deep-Sea Res. 37, 755–766.

Dickson, A.G., 1990b. Standard potential of the reaction: $AgCl(s) + ½H_2(g) = Ag(s) + HCl(aq)$, and the standard acidity constant of the ion HSO_4^- in synthetic sea water from 273.15 to 318.15 K. J. Chem. Thermodyn. 22, 113–127.

Dieckmann, G.S., Nehrke, G., Papadimitriou, S., Göttlicher, J., Steininger, R., Kennedy, H., Wolf-Gladrow, D., Thomas, D.N., 2008. Calcium carbonate as ikaite crystals in Antarctic sea ice. Geophys. Res. Lett. 35, L08501, http://dx.doi.org/10.1029/2008gl033540.

Dieckmann, G.S., Nehrke, G., Uhlig, C., Göttlicher, J., Gerland, S., Granskog, M.A., Thomas, D.N., 2010. Brief communication: Ikaite ($CaCO_3 \cdot 6H_2O$) discovered in Arctic sea ice. Cryosphere 4, 227–230.

DOE, 1994. Handbook of Methods for the Analysis of the Various Parameters of the Carbon Dioxide System in Sea Water; Version 2, Dickson, A.G., Goyet, C., (Eds.) (ORNL/CDIAC-74).

Fischer, M., Thomas, D.N., Krell, A., Nehrke, G., Göttlicher, J., Norman, L., Meiners, K.M., Riaux-Gobin, C., Dieckmann, G.S., 2013. Quantification of ikaite in Antarctic sea ice. Antarct. Sci. 25, 421–432.

Fransson, A., Chierici, M., Miller, L.A., Carnat, G., Shadnick, E., Thomas, H., Pineault, S., Papakyriakou, T.N., 2013. Impact of sea-ice processes on the carbonate system and ocean acidification at the ice-water interface of the Amundsen Gulf, Arctic Ocean. J. Geophys. Res. 118, 7001–7023.

Gleitz, M., Loeff, M.R.v.d., Thomas, D.N., Dieckmann, G.S., Millero, F.J., 1995. Comparison of summer and winter inorganic carbon, oxygen and nutrient concentrations in Antarctic sea ice brine. Mar. Chem. 51, 81–91.

Golden, K.M., Ackley, S.F., Lytle, V.I., 1998. The percolation phase transition in sea ice. Science 282, 2238–2241.

Hales, B., Chipman, D., Takahashi, T., 2004. High-frequency measurements of partial pressure and total concentration of carbon dioxide in seawater using microporous hydrophobic membrane contactors. Limnol. Oceanogr. Methods 2, 356–364.

Hare, A.A., Wang, F., Barber, D., Geilfus, N.X., Galley, R.J., Rysgaard, S., 2013. pH evolution in sea ice grown at an outdoor experimental facility. Mar. Chem. 154, 46–54.

IUPAC, 2002. Measurement of pH. Definition, standards, and procedures (IUPAC recommendations 2002). Pure Appl. Chem. 74, 2169–2200.

Khoo, K.H., Ramette, R.W., Culberson, C.H., Bates, R.G., 1977. Determination of hydrogen ion concentrations in seawater from 5 to 40 °C: standard potential at salinities from 20 to 40‰. Anal. Chem. 49, 29–34.

Liu, X., Patsavas, M.C., Byrne, R.H., 2011. Purification and characterization of meta-cresol purple for spectrophotometric seawater pH measurements. Environ. Sci. Technol. 45, 4862–4868.

Marion, G.M., 2001. Carbonate mineral solubility at low temperatures in the Na-K-Mg-Ca-H-Cl-SO_4-OH-HCO_3-CO_3-CO_2-H_2O system. Geochim. Cosmochim. Acta 65, 1883–1896.

Miller, L.A., Carnat, G., Else, B.G.T., Sutherland, N., Papakyriakou, T.N., 2011a. Carbonate system evolution at the Arctic Ocean surface during autumn freeze-up. J. Geophys. Res. 116, C00G04, http://dx.doi.org/10.1029/2011JC007143.

Miller, L.A., Papakyriakou, T.N., Collins, R.E., Deming, J.W., Ehn, J.K., Macdonald, R.W., Mucci, A., Owens, O., Raudsepp, M., Sutherland, N., 2011b. Carbon dynamics in sea ice: a winter flux time series. J. Geophys. Res. 116, C02028, http://dx.doi.org/10.1029/2009JC006058.

Miller, L.A., Fripiat, F., Else, B.G.T., Bowman, J.S., Brown, K.A., Collins, R.E., Ewert, M., Fransson, A., Gosselin, M., Lannuzel, D., Meiners, K.M., Michel, C., Nishioka, J., Nomura, D., Papadimitriou, S., Russell, L.M., Sørensen, L.L., Thomas, D.N., Tison, J.-L., van Leeuwe, M.A., Vancoppenolle, M., Wolff, E.W., Zhou, J., 2015. Methods for biogeochemical studies of sea ice: the state of the art, caveats, and recommendations. Elementa: Sci. Anthrop. 3 (10.12952/journal.elementa.000038). (000038).

Millero, F.J., 2009. Use of the Pitzer equations to examine the dissociation of TRIS in NaCl solutions. J. Chem. Eng. Data 54, 342–344.

Millero, F.J., Zhang, J.Z., Fiol, S., Sotolongo, S., Roy, R.N., Lee, K., Mane, S., 1993. The use of buffers to measure the pH of seawater. Mar. Chem. 44, 143–152.

Millero, F.J., Pierrot, D., Lee, K., Wanninkhof, R., Feely, R., Sabine, C.L., Key, R.M., Takahashi, T., 2002. Dissociation constants for carbonic acid determined from field measurements. Deep-Sea Res. I 49, 1705–1723.

Millero, F.J., Graham, T.B., Huang, F., Bustos-Serrano, H., Pierrot, D., 2006. Dissociation constants of carbonic acid in seawater as a function of salinity and temperature. Mar. Chem. 100, 80–94.

Millero, F.J., DiTrolio, B., Suarez, A.F., Lando, G., 2009. Spectroscopic measurements of the pH in NaCl brines. Geochim. Cosmochim. Acta 73, 3109–3114.

Munro, D.R., Dunbar, R.B., Mucciarone, D.A., Arrigo, K.R., Long, M.C., 2010. Stable isotopic composition of dissolved inorganic carbon and particulate organic carbon in sea ice from the Ross Sea, Antarctica. J. Geophys. Res. 115, C09005, http://dx.doi.org/10.1029/2009JC005661.

Notz, D., Worster, M.G., 2009. Desalination processes in sea ice revisited. J. Geophys. Res. 114, C05006, http://dx.doi.org/10.1029/2008JC004885.

Papadimitriou, S., Kennedy, H., Kattner, G., Dieckmann, G.S., Thomas, D.N., 2004. Experimental evidence for carbonate precipitation and CO_2 degassing during sea ice formation. Geochim. Cosmochim. Acta 68, 1749–1761.

Papadimitriou, S., Thomas, D.N., Kennedy, H., Haas, C., Kuosa, H., Krell, A., Dieckmann, G.S., 2007. Biogeochemical composition of natural sea ice brines from the Weddell Sea during early austral summer. Limnol. Oceanogr. 52, 1809–1823.

Papadimitriou, S., Thomas, D.N., Kennedy, H., Kuosa, H., Dieckmann, G.S., 2009. Inorganic carbon removal and isotopic enrichment in Antarctic sea ice gap layers during early austral summer. Mar. Ecol. Prog. Ser. 386, 15–27.

Papadimitriou, S., Kennedy, H., Norman, L., Kennedy, D.P., Thomas, D.N., 2012. The effect of biological activity, $CaCO_3$ mineral dynamics, and CO_2 degassing in the inorganic carbon cycle in sea ice in late winter-early spring in the Weddell Sea, Antarctica. J. Geophys. Res. 117, C08011, http://dx.doi.org/10.1029/2012JC008058.

Papadimitriou, S., Kennedy, H., Kennedy, P., Thomas, D.N., 2013. Ikaite solubility in seawater-derived brines at 1 atm and sub-zero temperatures to 265 K. Geochim. Cosmochim. Acta 109, 241–253 http://dx.doi.org/10.1016/j.gca.2013.01.044.

Papadimitriou, S., Kennedy, H., Kennedy, P., Thomas, D.N., 2014. Kinetics of ikaite precipitation and dissolution in seawater-derived brines at subzero temperatures to 265 K. Geochim. Cosmochim. Acta 140, 199–211 http://dx.doi.org/10.1016/j.gca.2014.05.031.

Pitzer, K.S., 1973. Thermodynamics of electrolytes. I. Theoretical basis and general equations. J. Phys. Chem. 77, 268–277.

Pratt, K.W., 2014. Measurement of pH_T values of Tris buffers in artificial seawater at varying mole ratios of Tris:Tris·HCl. Mar. Chem. 162, 89–95.

Robert-Baldo, G.L., Morris, M.J., Byrne, R.H., 1985. Spectrophotometric determination of seawater pH using phenol red. Anal. Chem. 57, 2564–2567.

Rysgaard, S., Glud, R.N., Sejr, M.K., Bendtsen, J., Christensen, P.B., 2007. Inorganic carbon transport during sea ice growth and decay: a carbon pump in polar seas. J. Geophys. Res. Oceans 112, C03016, http://dx.doi.org/10.1029/2006JC003572.

Rysgaard, S., Bendtsen, J., Delille, B., Dieckmann, G.S., Glud, R.N., Kennedy, H., Mortensen, J., Papadimitriou, S., Thomas, D.N., Tison, J.-L., 2011. Sea ice contribution to the air–sea CO_2 exchange in the Arctic and Southern Oceans. Tellus B 63, 823–830.

Rysgaard, S., Glud, R.N., Lennert, K., Cooper, M., Halden, N., Leakey, R.J.G., Hawthorne, F.G., Barber, D., 2012. Ikaite crystals in melting sea ice — implications for pCO_2 and pH levels in Arctic surface waters. Cryosphere Discuss. 6, 1015–1035 http://dx.doi.org/10.5194/tcd-6-1015-2012.

Rysgaard, S., Sogaard, D.H., Cooper, M., Pucko, M., Lennert, K., Papakyriakou, T.N., Wang, F., Geilfus, N.X., Glud, R.N., Ehn, J., McGinnis, D.F., Attard, K., Sievers, J., Deming, J.W., Barber, D., 2013. Ikaite crystal distribution in winter sea ice and implications for CO_2 system dynamics. Cryosphere 7, 707–718.

Takahashi, T., Sutherland, S.C., Sweeney, C., Poisson, A., Metzl, N., Tilbrook, B., Bates, N., Wanninkhof, R., Feely, R.A., Sabine, C., Olafsson, J., Nojiri, Y., 2002. Global sea-air CO_2 flux based on climatological surface ocean pCO_2, and seasonal biological and temperature effects. Deep Sea Res., Part II 49, 1601–1622.

UNESCO, 1983. Algorithms for computation of fundamental properties of seawater. Unesco Technical Papers in Marine Science. Vol. 44 (53 pp.).

Wren, S.V., Donaldson, D.J., 2012. Laboratory study of pH at the air-ice interface. J. Phys. Chem. C 116, 10171–10180.

Yamamoto-Kawai, M., McLaughlin, F.A., Carmack, E.C., Nishino, S., Shimada, K., 2009. Aragonite undersaturation in the Arctic Ocean: effects of ocean acidification and sea ice melt. Science 326, 1098–1100.

Yamamoto-Kawai, M., McLaughlin, F.A., Carmack, E.C., 2011. Effects of ocean acidification, warming and melting of sea ice on aragonite saturation of the Canada Basin surface water. Geophys. Res. Lett. 38, L03601, http://dx.doi.org/10.1029/2010gl045501.